Investigating the effects of water chemistry on carbonates and biota in a northern California spring region

A Thesis submitted to the faculty of
San Francisco State University
In partial fulfillment of
the requirements for
the Degree

Master of Science

In

Geoscience

by

Hannah Paulina Boelts

San Francisco, California

May 2021

Certification of Approval

I certify that I have read Investigating the effects of water chemistry on carbonates and biota in a northern California spring region by Hannah Paulina Boelts, and that in my opinion this work meets the criteria for approving a thesis submitted in partial fulfillment of the requirement for the degree Master of Science in Geoscience at San Francisco State University.

Yadira Ibarra Ph.D.
Assistant Professor,
Thesis Committee Chair

Erin Bray, Ph.D.
Assistant Professor

Leora Nanus, Ph.D.
Associate Professor

Investigating the effects of water chemistry on carbonates and biota in a northern California spring region

Hannah Paulina Boelts
San Francisco, California
2021

Abstract

Sedimentological observations and hydrogeochemical measurements of Ringtail Spring Creek, Felton, California were used to understand seasonal effects on groundwater chemistry and carbonate formation along a ~250 spring flow transect. Determining the effects of hydrochemistry and groundwater inputs on carbonate formation is significant for assessing the use of spring-associated carbonates (tufa) as an archive of regional climatic events. Ringtail Creek is a perennial spring that flows for an approximate 250 m stretch and exhibits a ~ 96 m elevation change from the outflow channel to the distal-most pool facies. This work presents hydrochemistry results from two sites (proximal and distal) and hydrochemical parameters measured *in situ* from three additional sites with distinct sedimentary facies along the flow path. Facies observations and hydrochemistry results suggest tufa deposition is strongly controlled by slope variations along the flow path, calcite saturation state, and water turbulence. Measurements of seasonal water parameters recorded from October 2019 to March 2021 indicate the following: (1) water temperature remains constant at the spring source (12.5-13.0°C), but exhibits strong

seasonal trends at the distal-most sites with warming to 13.5°C in the summer and cooling to 10.5°C in the winter, (2) pH ranges from 7.3 to 8.0 at the source and all sites exhibit a rise in pH irrespective of the season, and (3) there is a notable rise in calcite saturation state from the source to the distal-most pool which reflect observations of modern carbonate deposition in the distal-most sites. Hydrochemistry data collected in the winter of 2020-2021 nearly doubles in concentration for organic carbon (TOC and DOC), and the redox potential of the waters measured *in situ* reflect the lowest values recorded. We attribute these changes to an influx of organic carbon resulting from the CZU Lightning Complex Fire which burned the Ringtail Spring Creek catchment from August 16, 2020 to September 22, 2020 signifying a relatively rapid groundwater infiltration response following the first post-fire rainfall of the winter season. This work represents a first look at the effects of spring chemistry on tufa deposition to serve as a baseline and reference for future analyses on currently-forming and ancient tufa deposits in the region.

Acknowledgements

First, I want to thank my advisor, Yadira Ibarra, for always pushing me to be my best, supporting me, and for providing me with all the necessary tools to complete my degree. I would also like to thank my committee members Erin Bray and Leora Nanus. Jason Gurdak was instrumental with assistance with the water chemistry analyses. I would like to thank the Earth and Climate Sciences department at San Francisco State University for awarding me the Professor Emeritus Dave Dempsey and Rebecca Douglass Scholarship. I would also like to thank Pascal Broca and the California State Parks for access to the spring. Finally, thank you to Dr. Daniel Snow and the Nebraska Water Center for analyzing the water samples for the water chemistry data. This research was conducted on the land of the Ohlone Tribe in Santa Cruz, CA.

Table of Contents

List of Tables

List of Figures

Introduction

As sedimentological deposits of geochemical conditions that originate in the subsurface (e.g., groundwater), carbonate spring deposits can be an important archive of hydrogeological conditions in areas that are prone to drought or floods (Quade et al., 2017; Andrews, 2006; Arenas et al., 2014; Cappezuoli et al., 2014). The northern California coast is a particularly vulnerable area where groundwater is already overdrawn to sustain population centers and agriculture (Jasechko and Perrone, 2021; Gurdak et al., 2009; Gurdak et al., 2017). To implement a sustainable water resource policy, a thorough understanding of regional climate history is essential to understand natural baselines of hydroclimatic variability and water availability. Understanding the processes that control carbonate formation in springs in the northern California area is key to unlocking the palaeohydrological records of carbonates associated with those springs as well as determine the paleoenvironmental significance of tufa deposits that are no longer active. However, most springs in the coastal California region are intermittent, or ephemeral, meaning that they dry up at some point during the year due to a lack of groundwater recharge to the aquifer (White, 2010). In this study, I investigate the effects of spring water chemistry in a rare *perennial* spring in northern coastal California on carbonate formation downstream. This seasonal study of a perennial cold spring allows for a rare glimpse into how springs behave in the cold, wet months as well as the warm, relatively drier months. Determining the effects of hydrochemistry and groundwater inputs on carbonate formation is significant for assessing the use of ancient spring-associated carbonates in the Santa Cruz region as an archive of regional climatic events.

Background

Mechanisms of Tufa Formation

Tufa is a carbonate deposit that forms from ambient temperature spring water (Ford and Pedley, 1996). Since the CO_2 associated with the groundwater that feeds tufa deposits is meteoric in origin (derived from the atmosphere and soil zone), some workers also refer to tufa deposits at meteogene spring carbonates (Ford and Pedley, 1996). Carbonate deposition results from a series of processes that involve infiltration, dissolution, saturation, subsurface transport, emergence, and precipitation (Capezzuoli et al., 2014). As rainwater percolates through the soil horizon, it becomes enriched in soil CO_2. With continued subsurface transport, the CO_2-rich groundwater reacts with the carbonate bedrock causing the carbonate to dissolve and thereby enriching the groundwater with calcium and bicarbonate ions by the following reaction:

Reaction 1: $CaCO_3 + CO_2 + H_2O \rightarrow Ca^{2+} + 2(HCO_3)^-$

During episodes of accelerated groundwater flow, water will emerge to the surface at a spring orifice and descend via gravity into areas of lower elevation. Spring carbonate precipitation will result by running reaction 1 to the left. Several variables drive reaction 1 to the left, leading to increased CO_2 degassing and subsequent carbonate precipitation: water temperature, air temperature, turbulence, discharge size, and biology (e.g., photosynthesis). Of these processes, the amount of turbulence that the flowing water experiences is often cited as the leading factor driving carbonate precipitation (Pentecost, 2005; Andrews, 2006). Therefore, areas along the flow path that experience accelerated flow and agitation (cascade and terrace facies) are usually characterized by thicker carbonate accumulations. With increasing distance from the spring orifice, supersaturation with respect to carbonate decreases resulting in less carbonate precipitation.

An increasing body of data from active tufa sites (Campos, R., Goni, J., Treibs, 1977; Ford and Pedley, 1996) has revealed that in some cases, the greatest calcium carbonate accumulations occur in the immediate vicinity of photosynthesizers (macrophytes, microphytes, and cyanobacteria). Tufa deposits can preserve fossils of cyanobacteria, algae, and other small invertebrates, which allows for observations of microbe-mineral interactions of recently lithified deposits (Andrews, 2006; Capezzuoli et al., 2008; Gradziński, 2010). For my undergraduate senior project, I investigated the microstructure of tufa deposits in Ringtail Spring Creek to assess the role of biology (diatoms) on the resulting carbonate textures. Results from that research show that diatoms can contribute to lasting changes in the carbonate texture and porosity by secreting exopolymers (Boelts et al., 2020), but metabolic effects on carbonate chemistry were not assessed.

In addition to serving as natural laboratories to study microbe-mineral interactions, terrestrial carbonate springs are important archives of the environmental setting in which they form (Pedley, 2003; Arenas et al., 2014). Tufa is a spring-sourced terrestrial carbonate deposit that can record changes in climate and hydrology of the source waters at seasonal to multidecadal timescales (Arenas et al., 2000, 2015; Minissale et al., 2002; Andrews, 2006; Gradziński, 2010; Ibarra et al., 2015). Analyzing the different textures and thicknesses of the carbonate laminations in tufa deposits can help to decipher the time of year the tufa was formed and determine its growth rate (Minissale et al., 2002; Gradziński, 2010). Geochemical studies of carbonate spring water in areas that have active tufa accretion have revealed records of seasonal and interannual environmental conditions and can be used to track short-term environmental changes through variations in their lamina thickness (Kawai et al., 2009; Brasier et al., 2010). A majority of the present fluvial tufa analyses use stable-isotope geochemistry and hydrochemistry to understand carbonate formation and there are some studies that use biological evidence to understand the role that microorganisms (e.g., algae) play in tufa formation (Arenas et al., 2014).

Tufa as a paleoclimate proxy

Tufa deposits only form when the water table is sufficiently drowned to (1) sustain surface water flow and (2) promote dissolution in the subsurface to concentrate the water with bicarbonate (Pentecost, 2005). Therefore, tufa growth is dependent on water availability (precipitation), which is a direct consequence of wet climatic conditions. The presence of fossil tufa is often used to infer wetter climate in areas that today are characterized by more arid conditions (Cremaschi et al., 2010).

Studies on modern tufa deposition have shown that some tufa deposits display coupled laminations that represent seasonality. Most Holocene tufa records however, are not laminated and oftentimes the dynamic depositional nature of most tufa deposits results in porous and only partially laminated deposits. Despite the lack of laminations, useful paleoclimatic signals have been successfully extracted from tufas (Garrett, 2004; Capezzuoli et al., 2014; Rabassa, 2021).

The most commonly used proxies to infer paleoclimatic change are stable isotopes of carbon and oxygen (Garrett, 2004; Capezzuoli et al., 2014; Rabassa, 2021). The characteristic stable isotopic signature of tufas that develop under arid conditions, could be distinguished from those that form in the presence of soils which imply wetter conditions (Pentecost, 2005). However, the majority of these studies have been conducted on European tufas (Arenas et al., 2000; Andrews, 2006).

Seasonal effects of water chemistry on carbonate precipitation

Carbonate precipitation in fluvial tufa settings has been shown to be more prevalent in the spring season due water availability and accelerated dissolved ion removal from the underlying bedrock (Arenas et al., 2014, 2015). The saturation state of calcite (SI) becomes elevated during the spring season in areas that experience turbulent flow downstream like the cascade facies. Turbulence at cascade facies allow for the rapid release of carbon dioxide through degassing which causes the water to become supersaturated with calcium carbonate and favoring carbonate precipitation. However, the carbonate saturation state of the water is typically reduced with distance from the source (Capezzuoli et al., 2014) as the tufa develops along the flow path. At Ringtail Spring Creek, most of the tufa observed along the flow path is concentrated between the cascade and distal-most pool. There are no large tufa accumulations after the distal-most pool, likely owing to a decrease in carbonate saturation due to distance from the source (Arenas et al., 2015). Furthermore, tufa precipitation has been shown to dominate in the wet season, in response to higher flow rates (Gradziński, 2010). Dissolved ions can be used to understand how the aquifer changes over time. Specifically, the Ca/Mg ratio is commonly used to infer relative residence times, whereby higher Ca/Mg ratio suggests longer residence times of water in the aquifer.

The Santa Cruz California region contains several groundwater aquifers that are composed of limestone and marble which feed nearby springs and streams. Active streams in the region are associated with massive deposits of the ancient tufa (Ibarra and Sanon, 2019) deposited at time when the region likely sustained greater groundwater recharge. In order to understand the conditions that would have formed the large, inactive tufa deposition to use as a record of regional past pluvial (or wet events), it is important to determine a baseline for the semi-arid conditions in which modern tufa accumulates today. The goal of this work is to characterize the carbonate facies and hydrochemistry of the spring water of Ringtail Spring Creek, a perennial spring that flows in the Santa Cruz Mountains of California. Determining the effects of hydrochemistry and groundwater inputs on carbonate formation is significant for assessing the use of ancient spring-associated carbonates in the Santa Cruz region as an archive of regional climatic events.

Geologic and Environmental Setting

Ringtail Creek is a tufa-precipitating spring in the Fall Creek unit of Henry Cowell State Park in Felton, California (Boelts et al., 2020)(Fig. 1). The bedrock is composed of Mesozoic or Paleozoic schist and marble (Kellman, 2003; Brabb, 1997)(Figure 2). The Paleozoic marble was mined in the Santa Cruz region between 1870 and 1919 for the production of lime in the cement industry (Kellman, 2003). The tufa-precipitating spring is likely sourced from bicarbonate-rich groundwater derived from the Paleozoic marble. The spring carbonates of Ringtail Creek occur west of the Ben Lomond fault on Ben Lomond Mountain (Boelts et al., 2020), and are a part of the San Lorenzo Watershed which encompasses the California Coastal Aquifer (Figure 3;

USGS). The spring overlies what is considered a 'hard rock' hydrogeologic unit because the groundwater comes from aquifers in granitic, metamorphic, or lithified sedimentary rocks, rather than from sediments in groundwater basins. Groundwater recharge to hard-rock aquifers is through direct precipitation infiltration ("California Department of Water Resources," 2014).

Felton California experiences a Mediterranean climate that is characterized by dry summers and cold, wet winters. Precipitation occurs as rain during winter and early spring and as fog cover in the summer months. This climate is conducive to redwood forests which dominate in the catchment of Ringtail Creek. The air temperature is moderate year-round, where the average annual high temperature is 22.8°C and the average annual low temperature is 3.9°C (usclimatedata.com). The average annual precipitation in Felton, CA is 22.7 cm. Ringtail Creek is a rare perennial cold spring in coastal northern California and its association with carbonate formation presents the unusual opportunity to investigate the seasonal hydrologic changes that can influence (1) carbonate growth and (2) the microorganisms that are present in the spring.

Methods

In situ water quality measurements were acquired using a YSI ProDSS Multiparameter Water Quality Meter at five different sampling locations along the spring transect: source, cascade, first pool, flag pool, oncoid pool (Figs. 4-5). Measurements were taken seven different times during a two-year period (Table 1). The YSI probe measures temperature, dissolved oxygen, conductivity, salinity, pH, and oxygen redox potential (Table 1). The probe is inserted into the water at each location and the information is recorded after approximately 15-30 seconds. Facies observations were carried out at the five measurement sites along the spring flow transect. Observations include carbonate presence, flow characteristics, and carbonate facies descriptions.

Water samples were collected four times during the period between October 2019 to February 2021 (Table 2 and Table 3). The water samples were collected at the source of the cold spring and at the distal-most carbonate forming pool (oncoid pool) (Figs. 4-5). The samples are held in plastic and glass bottles. Some of the samples are filtered through a 45-micron filter and all the samples are refrigerated or frozen. Unfortunately, the COVID-19 pandemic prevented additional planned sampling times and limited the water collection dates to the winter months. However, the water quality measurements encompass some of the summer months that are lacking in the water chemistry data. Upon collection, water samples were kept refrigerated or frozen and sent to the Nebraska Water Center for analysis of major anions, major cations, dissolved oxygen content (DOC), total organic carbon (TOC), ^{13}C in total organic carbon, silica, potentiometric titration of alkalinity, tritium, water hardness by calculation, total dissolved solids (TDS), and dissolved elements in water (Table 2 and Table 3). The calcite and silica saturation (Table 2) state were determined using PHREEQC software (David Parkhurst, Apello, 2014). To monitor the organics and biota in the spring, I measured DOC, TOC, ^{13}C in TOC, and silica (a source for diatom frustules). I used these parameters to understand how organics and biota behave throughout the year. I was particularly interested in diatoms, which thrive in the summer when there is higher levels of sunlight, so I expected that the silica levels would also be highest during the summer (Pfister et al., 2017). The source for silica is the schist in the bedrock, which is likely enhanced during accelerated recharge events such as storms in the winter and spring months. Determining silica variability will help inform the use of silica in the formation of a diatom's frustule.

Results

Description of Facies and water collection sites

There is carbonate accumulation along a ~250 m transect of the spring that displays a variety of facies (m-scale morphology): channel, pool, and paludal (Capezzuoli et al., 2014; Boelts et al., 2020). The spring flow transect undergoes approximately 96 meters of elevation change from the source of the spring to the most distal carbonate precipitating pool (Figs. 4-5). The first ~45 m stretch from the outflow channel to the cascade facies does not contain evidence for carbonate formation or evidence for ancient tufa accumulation (Fig. 4A). The elevation difference from 470 m to ~420 m is gradual with few to no drastic slope variations. The first drastic steep elevation change happens immediately before the cascade site (Fig. 4B) at ~425 m. This area exhibits at least two ~1.5 m (near vertical) drops in elevation (Fig. 4B). The cascade site is the first facies along the spring flow transect that contains carbonate accumulation in the spring channel as well as up to two meters away from the channel along the spring bank. The next sampling site (pool 1; Fig. 4C) occurs at 147 m from the spring source. *In situ* carbonate accumulation at this site was not discernable due to vegetation cover but flow was present at every sampling period in a pool that is approximately 20 cm deep. The second pool at approximately 200 m from the source (Fig. 4D) contains a ~50 cm near vertical change in elevation. Tufa can is present along the channel as well as in the splash zone terrace face (Fig. 4D). The distal-most sampling site is the oncoid pool at ~252 m from the source (Fig. 4E).

Carbonate accumulates along the channel prior to and at the base of the drop of a ~30 cm terrace face (Fig. 4E). The shallow (~10 cm deep) pool at the base of the face accumulates carbonate coated grains (oncoids) which were the focus of my undergraduate research (Boelts et al., 2020).

Water Quality – Field Data

Seasonal field data are reported in Table 1 and Figures 6-11. Fall and winter water temperature values get colder with distance from the source to the distal-most point (oncoid pool) (Table 1, Fig. 6). The spring and summer water temperatures increase with distance from the source to the oncoid pool (Table 1, Figs. 5- 6). The temperature at the source of the spring remains relatively constant year-round with a temperature of 12.6°C - 12.8°C. The pH values at the source are lowest in January, February, and May of 2020 with values ranging from 7.2 to 7.4. After May of 2020, the pH values at the source increase to approximately 7.8 (Table 1, Fig. 7). There is a notable increase in pH from the lowest values at the source, to higher values at the cascade (~8.2), and finally the pools seem to stay quite stagnant (Table 1, Fig. 7). March of 2021 has the highest values for pH across the entire sampling period (Table 1, Fig. 7). When comparing temperature versus pH at the source, the temperature stays constant and the pH appears to change seasonally (Table 1, Fig. 8). At the cascade and distal-pool facies, the temperature decreases or increases by approximately one to two degrees, whereas the pH remains relatively constant (Table 1, Fig. 8).

The dissolved oxygen (DO) values follow a consistent pattern, whereby the lowest values are at the source, there is a steep increase at the cascade, and from the cascade through to the distal pools the values remain relatively constant (Table 1, Fig. 9). The highest values for DO were measured in January 2020 and the lowest values were in July 2020; the rest of the months yield similar DO values (Table 1, Fig. 9). The oxygen redox potential (ORP) values are plotted in Figures 10 and 11. ORP values range from 100 to 340 mV with no clear seasonal or proximal to distal patterns (Table 1, Fig. 10). January and February of 2020 yield the highest ORP values (Table 1, Fig. 11). The conductivity data ranges from 13.8 – 417.8 uS/cm but does not show a distinct seasonal or proximal to distal pattern (Table 1). Salinity values remain consistent at or below 0.2 ppt (Table 1).

Water Chemistry – Water Samples

$CaCO_3$ and silica values had a consistent pattern where the source yielded higher values than the distal-most pool, regardless of the time of year/season (Table 2). There was also a consistent pattern with the calcium levels of the spring water where the source yielded a higher value than the oncoid pool yield (Table 2, Fig. 4, Fig. 12-13). K, Mg, and Na remained fairly constant throughout the whole year at both sampling sites. The dissolved organic carbon (DOC) and total organic carbon (TOC) values demonstrate an approximate doubling from 0.68 mg C/L for DOC and 1.37 mg C/L for TOC in January 2020 to 2.32 mg C/L for DOC and 3.07 mg C/L for TOC in February 2021 (Table 3 and Fig. 14). The dissolved inorganic carbon (DIC), DOC, total inorganic carbon (TIC), and TOC values remain relatively constant throughout the entire sampling period. DIC, DOC, TIC, and TOC values were slightly higher at the source compared to the distal-most pool, but overall do not experience notable variability (Table 3). Along with most of the water chemistry values yielded in this study, the alkalinity values were also higher at the source than they were at the oncoid pool. The piper diagram in Figure 15 illustrates the calcium bicarbonate nature of the spring waters. Figure 16 shows that silica concentrations do not exhibit a distinct temporal or spatial pattern.

Saturation Index

The saturation index of calcite ranged from -0.13 to 0.57 at the source (HCP) and -0.44 to 0.96 at the oncoid pool (HCD) of Ringtail Creek (Table 2 and Fig. 17). The saturation index of silica ranged from -0.5 to -0.61 at HCP and -0.58 to -0.59 at HCD (Table 2).

Discussion

Water Quality

Spring water temperatures ranged from 10.4 to 13.6 degrees Celsius, which is within the typical range of water temperature for a tufa producing spring (Capezzuoli et al., 2014; Kano et al., 2019). During the winter and fall, the water temperature gets colder with distance from the source and during the spring and summer the water temperature gets warmer with distance from the source (Table 1, Fig. 4, Fig. 5). This clear seasonal temperature change indicates that the spring water temperature is affected by ambient air temperature conditions along the flow transect. In addition, the consistent temperature of the water at the source demonstrates that the spring outlet is not affected by seasonal changes as has been observed elsewhere (Arenas et al., 2014). While most sampling dates follow a summer warming, and winter cooling trend, there is an anomaly to this pattern in the February 2020 and February 2021 season. All winter months show decreasing temperature from the source to the oncoid pool, but water temperature during February 2020 is approximately 1.2°C - 1.5°C warmer than February 2021 at all sampling locations except for the source (Table 1). In the absence of long-term water temperature data from this site, the veracity of this observation as an anomaly remains to be seen.

The pH values are consistent with observations of carbonate precipitation along the spring (Arenas et al., 2014, 2015; Kano et al., 2019). The values were in the neutral zone (~7.0) at the source and exhibit an increase at the cascade and through to the pool facies (Table 1, Fig. 7). Our field observations indicate the spring source lacks carbonate formation and the first site with modern carbonate accumulation is at the cascade (Fig. 4). Carbonate accumulation is also observed downstream at the flag and oncoid site (Table 2, Fig. 4).

The DO values decrease from the winter to the summer, while the temperature increases from the winter to the summer, suggesting that there was an increase in biogeochemical reactions (e.g,. photosynthesis) from the winter to the summer which agrees with the observation that diatoms thrive in the summer (Kumar et al., 1997; Boelts et al., 2020). The oxygen redox potential (ORP) values do not show strong facies (or longitudinal) trends from site to site. The two highest ORP values are from two winter months in the year 2020 (Jan and Feb; Figs. 10-11). However, the subsequent year yielded lower ORP values starting from November 2020 through to January and February of 2021 (Fig. 11). We attribute this difference to the effects of the CZU Lightning Complex Fire which burned through the Ringtail Creek area from August 16, 2020 through to September, 22, 2020. Oxygen redox potential measures the oxidizing or reducing potential of a water sample. The lower post-fire ORP values in the winter of 2020-2021 may be a signal of rapid oxidation resulting from an increase of dissolved nutrients to the groundwater system. In particular, February and March 2021 water measurements had the lowest ORP values at the source and these samples were collected after the first post-fire rainfall implying increased runoff and infiltration in the Ringtail Creek catchment.

Water Chemistry

Differences in water chemistry values at the source and the distal-most pool can be attributed to pure spring water (source) versus spring water with multiple inputs (distal-most pool) such as surface water runoff and other small inputs that feed into Ringtail Creek (Arenas et al., 2014). The DOC and TOC values doubled after the CZU Lightning Complex Fire burned through the research site (Table 3, Fig. 14). This is likely due to carbon from the ash seeping into the groundwater and from transport via surface water flow. The surface water flow has the ability to carry the excess carbon to the catchment, resulting in higher DOC and TOC values. There was a continuous decrease in alkalinity and calcium content from the source to the distal-most pool throughout the year (Fig. 12), suggesting that there was carbonate sedimentation along the spring transect (Arenas et al., 2014). Although we were not able to collect water samples in the late spring and early summer, there is an increase of DOC from November to February which suggests that DOC would continue to rise throughout the spring and summer, supporting the hypothesis that diatoms thrive in the warmer periods (Henrichs, 1987; Kumar et al., 1997; Boelts et al., 2020). Calcium is the most abundant cation in Ringtail Creek throughout the year (Table 2). Calcium values at the source yield higher values than at the oncoid pool which is likely attributed to greater carbonate formation at the distal-most point of Ringtail Creek (Fig. 12) (Swart, 2015). Also, the high levels of calcium (and low levels of sodium) indicate that the sub-surface water is leaching carbonate from the underlying limestone (Table 1) (Kokh et al., 2017).

Saturation Index

During all the sampling periods, the source yielded lower numbers for the calcite saturation index than at the oncoid pool. The observed increase in calcite saturation is likely due to CO_2 degassing with flow and turbulence downstream (Kawai et al., 2009; Brasier et al., 2010; Gradziński, 2010). The loss of CO_2 from the water in areas of high energy allows for tufa sedimentation to occur (Arenas et al., 2015). The saturation index of calcite was lowest and undersaturated in October of 2020 at both the source (HCP) and the oncoid pool (HCD) (Table 3), however, we note that this sampling period did not include anions which may have contributed to the low calcite SI values. All the rest of the sampling dates yielded saturation index values that favored calcite precipitation in the spring, with November of 2020 at the oncoid pool yielding the highest value (Table 2). Along with the higher saturation index values at the oncoid pool, the pH values are also more basic at the oncoid pool than at the source, indicating favorable conditions for carbonate deposition (Table 2) (Arenas et al., 2015).

Conclusion

Sedimentological and hydrogeochemical conditions of Ringtail Spring Creek in Santa Cruz California were measured and monitored at five sites along the spring flow transect from October 2019 to March 2021. Results show that water temperature remains relatively constant at the spring source (12.5-13.0°C), but exhibits strong seasonal trends at the distal-most sites with warming to 13.5°C in the summer and cooling to 10.5°C in the winter,) pH ranges from 7.3 to 8.0 at the source and all sites exhibit a rise in pH irrespective of the season, and there is a notable rise in calcite saturation state from the source to the distal-most pool which reflect observations of modern carbonate deposition in the distal-most sites. Data collected in the winter of 2020-2021 nearly doubles in concentration for organic carbon (TOC and DOC), and the redox potential of the waters measured in situ reflect the lowest values recorded, which are attributed to the effects of the CZU Lightning Complex Fire which burned the Ringtail Spring Creek catchment from August 16, 2020 to September 22, 2020. The temperature and chemical characteristics (e.g., calcium bicarbonate character) of the spring source remains remarkably constant through time suggesting the dominant factors controlling tufa formation downstream are governed by the temporal and spatial evolution of the surface waters along the spring flow transect. Changes in slope along the flow path are consistently associated with tufa deposition. This data presents a starting point upon which additional monitoring, particularly more data during the summer months which was not possible here due to the COVID 19 pandemic, will help determine which sites along the flow path may preserve the most complete information in the tufa sedimentary record. Determining the effects of hydrochemistry and groundwater inputs on carbonate formation is significant for assessing the use of ancient spring-associated carbonates in the Santa Cruz region as an archive of regional climatic events.

Table 1. Water Quality

Sample Location	Date	Elevation (m)	Temp. (C)	DO %L	DO mg/L	DO ppm	SPC - uS/cm	ohm - cm	SAL - ppt	pH	ORP mV
Source (HCP)	1/14/20	472	12.7	74.3	7.53	7.53	409.7	3191.1	0.2	7.29	257.8
Cascade	1/14/20	435.34	12.1	99.8	10.28	10.28	102.1	12987	0.05	8.21	219.5
1st Pool	1/14/20	418.42	10.7	99.6	10.67	10.67	377.7	3645.9	0.18	8.31	231.1
Flag Pool	1/14/20	381.69	10.6	99.6	10.7	10.7	377.9	3651.1	0.18	8.26	232.9
Oncoid Pool (HCD)	1/14/20	376.62	10.4	99.8	10.78	10.78	313.4	4423.8	0.15	8.3	230.3
Source (HCP)	2/28/20	472	12.7	77.1	7.82	7.82	41.8	31266.7	0.02	7.3	341.6
Cascade	2/28/20	435.34	12.9	98	9.9	9.9	405.1	3211.1	0.2	8.04	330.2
1st Pool	2/28/20	418.42	12.1	99.6	10.29	10.29	388	3417.1	0.19	8.19	279.6
Flag Pool	2/28/20	381.69	12.1	99.2	10.27	10.27	387.1	3428.4	0.19	8.14	288.6
Oncoid Pool (HCD)	2/28/20	376.62	12.2	98.4	10.17	10.17	46.8	7945.9	0.02	8.21	326.5
Source (HCP)	5/2/20	472	12.7	75.2	7.6	7.6	411.1	3180.6	0.2	7.48	162.6
Cascade	5/2/20	435.34	12.7	99.2	10.06	10.06	403.8	8236.8	0.2	8.26	142.6
1st Pool	5/2/20	418.42	12.8	99	10.09	10.09	387.9	3364.8	0.19	8.31	159
Flag Pool	5/2/20	381.69	12.8	98.6	10.05	10.05	384.2	3396.6	0.19	8.24	169.3
Oncoid Pool (HCD)	5/2/20	376.62	12.9	99.1	10.09	10.09	380.9	3417.8	0.18	8.31	195.5
Source (HCP)	7/9/20	472	12.8	78.9	7.91	7.91	407.3	3204.8	0.2	7.79	157.6
Cascade	7/9/20	435.34	13	98.3	9.82	9.82	409	3169.3	0.2	8.25	140.9
1st Pool	7/9/20	418.42	13.4	98.3	9.81	9.81	389.9	3297.3	0.19	8.33	159.7
Flag Pool	7/9/20	381.69	13.4	97.9	9.77	9.77	60.2	21311.5	0.03	8.25	157.5
Oncoid Pool (HCD)	7/9/20	376.62	13.6	98.1	9.76	9.76	13.8	92598.8	0.01	8.29	150.2
Source (HCP)	11/14/20	472	12.7	76.8	7.79	7.79	417.8	3130.5	0.2	7.96	158
Cascade	11/14/20	435.34	12.6	93.1	9.47	9.47	415.9	3151.3	0.2	8.11	135.5
1st Pool	11/14/20	418.42	11.7	97	10.15	10.15	382.4	3505.5	0.18	8.36	111.8
Flag Pool	11/14/20	381.69	11.7	96.6	10.13	10.13	381.2	3521.3	0.18	8.38	98
Oncoid Pool (HCD)	11/14/20	376.62	11.6	96.1	10.1	10.1	301.9	4449.9	0.14	8.37	129.8
Source (HCP)	2/12/21	472	12.6	74.3	7.5	7.5	415.1	3155.3	0.2	7.84	113.9
Cascade	2/12/21	435.34	N/A								
1st Pool	2/12/21	418.42	10.9	96.6	10.23	10.23	385	3554.7	0.19	8.3	135.2
Flag Pool	2/12/21	381.69	10.8	96.6	10.28	10.28	363.4	3777.4	0.18	8.25	129
Oncoid Pool (HCD)	2/12/21	376.62	10.7	95.7	10.22	10.22	404	3409.5	0.2	8.24	113.4
Source (HCP)	3/6/21	472	12.6	73.5	7.44	7.44	417.2	3141.6	0.2	7.95	116.1
Cascade	3/6/21	435.34	12.1	96.5	9.92	9.92	410.7	3235.1	0.2	8.25	91.7
1st Pool	3/6/21	418.42	10.7	96.7	10.3	10.3	385.9	3562	0.19	8.42	117.6
Flag Pool	3/6/21	381.69	10.6	96.1	10.28	10.28	21.9	62852.7	0.01	8.52	101.6
Oncoid Pool (HCD)	3/6/21	376.62	10.5	95	10.2	10.2	389.7	3550.7	0.19	8.53	109.7

Table 1. Water quality data from the five different sampling locations (Source, Cascade, 1st Pool, Flag Pool, Oncoid Pool) along Ringtail Creek.

Table 2. Water Chemistry

Sample ID	Sample Date	Ca^{2+} (mg/L)	K^{+} (mg/L)	Mg^{2+} (mg/L)	Na^{+} (mg/L)	Cl^{-} (mg/L)	F^{-} (mg/L)	SO_4^{2-} (mg/L)	Silica (mg/L)	TDS (mg/L)	pH	Alk as HCO_3^- (mg/L)	Alk as $CaCO_3$ (mg/L)	$SI_{calc.}$	SI_{silica}
HCP 102219	10/22/19	48.8	1.84	9.39	5.55				23.0		7.37	261	214	-0.13	-0.6
HCD 102219	10/22/19	42.3	1.81	9.39	5.57				23.2		7.13	267	219	-0.44	-0.59
HCP 011420	1/14/20	54.7	1.84	9.62	5.63	8.21	0.203	6.44	29.1	16.9	7.88	284	233	0.44	-0.5
HCD 011420	1/14/20	52.8	1.82	9.35	5.59	8.25	0.192	6.33	23.4	14	8.19	216	177	0.59	-0.58
HCP 111420	11/14/20	69.0	2.42	8.70	6.41	8.49	0.066	6.79	22.6	17.3	7.96	253	208	0.57	-0.61
HCD 111420	11/14/20	62.2	2.08	8.93	6.29	8.66	0.0611	7.3	23.7	10	8.46	235	192	0.96	-0.59
HCP 21221	2/12/21	61.7	1.78	16.3	5.96	9.32	0	7.8	24.1	24.3	7.61	248	204	0.16	-0.58
HCD 21221	2/12/21	57.1	1.76	16.3	5.90	10.2	0	8.14	23.2	23.5	8.47	235	192	0.91	-0.59

Table 2. Water chemistry data from source (HCP) and distal-most pool (HCD) along Ringtail Creek.

Table 3. Organic Carbon

Sample ID	Sample Date	DIC (mg C/L)	DOC (mg C/L)	TIC (mg C/L)	TOC (mg C/L)
HCP 102219	10/22/19		0.734		2.13
HCD 102219	10/22/19		0.758		1.97
HCP 011420	1/14/20		0.68		1.37
HCD 011420	1/14/20		1.14		-
HCP 111420	11/14/20	28.5	1.05	34.4	1.71
HCD 111420	11/14/20	27.4	1.41	33.4	1.75
HCP 21221	2/12/21	36.5	2.32	47.5	3.07
HCD 21221	2/12/21	31.3	2.02	44.0	2.85

Table 3. Organic carbon data from the source (HCP) and distal-most pool (HCD) along Ringtail Creek.

Figure 1. Map of Santa Cruz

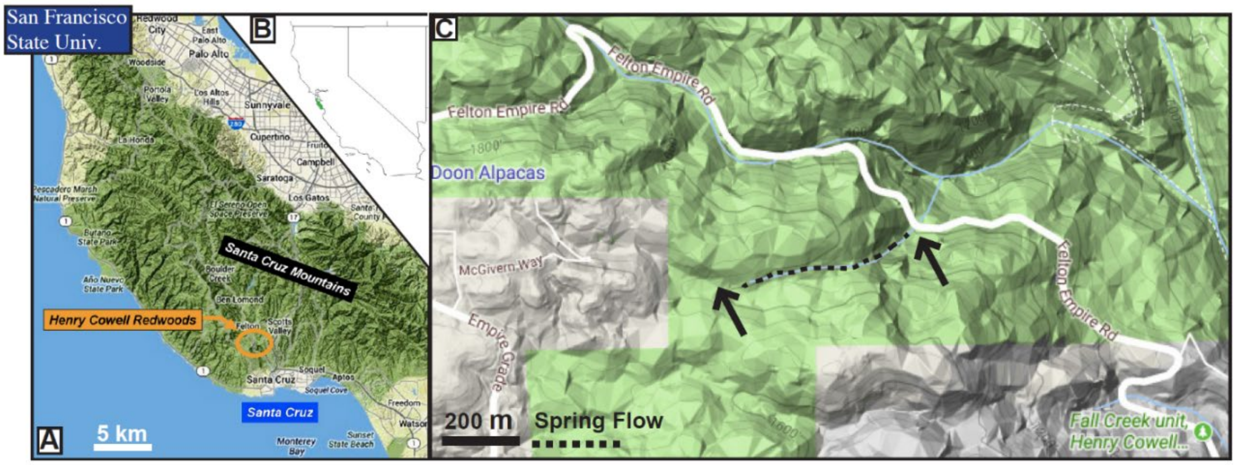

Figure 1. A. Map demonstrating the location of the study area in Santa Cruz County. B. Zoomed out map of the state of California. C. Zoomed in map of the study area, Ringtail Creek.

Figure 2. Geologic map of Santa Cruz County

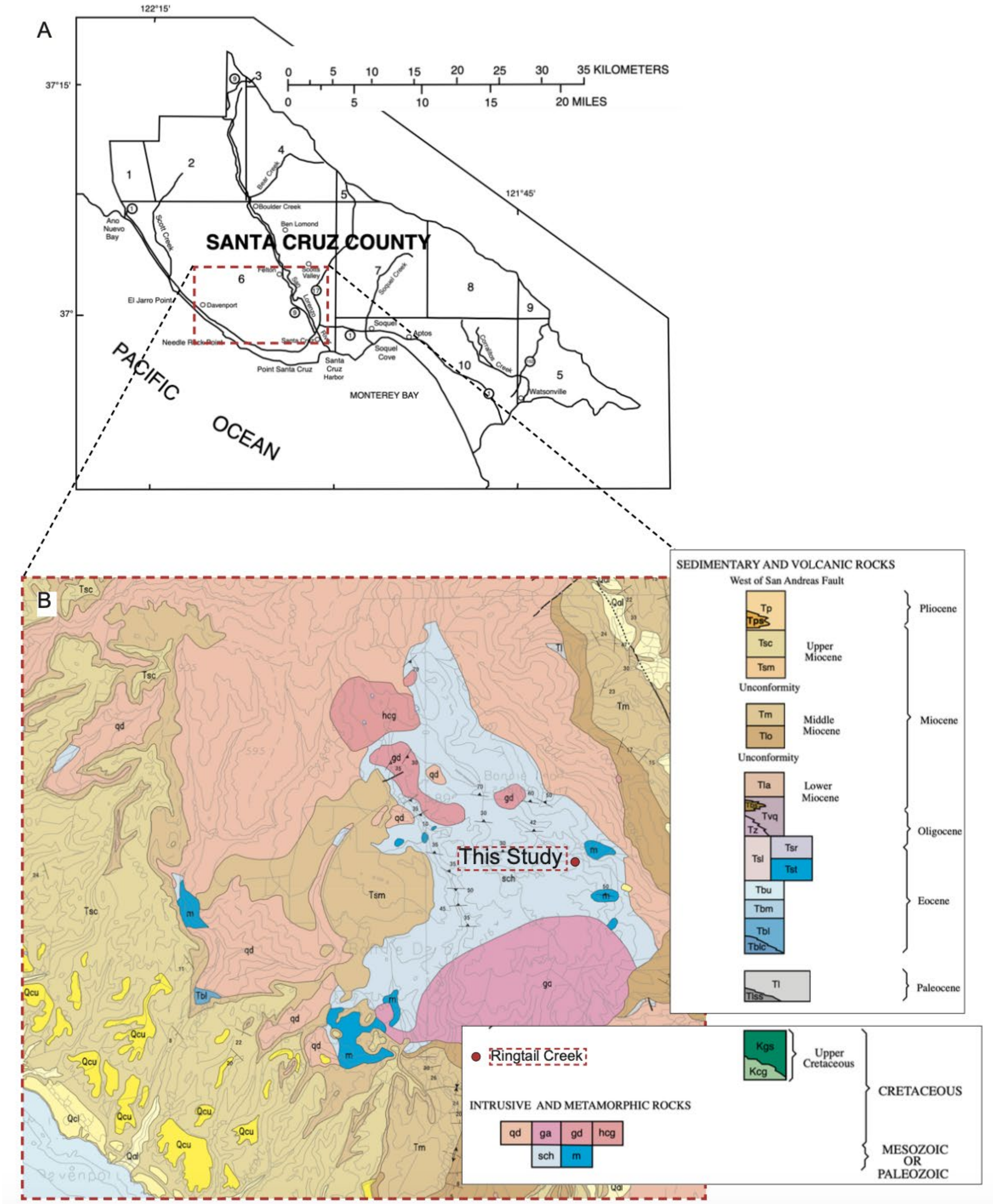

Figure 2. Geologic map of Santa Cruz, California (after Brabb, 1997). Relevant lithologies include: m, marble; sch, metasedimentary rocks mainly pelitic schist and quartzite; qd, quartz diorite.

Figure 3. Watershed Map

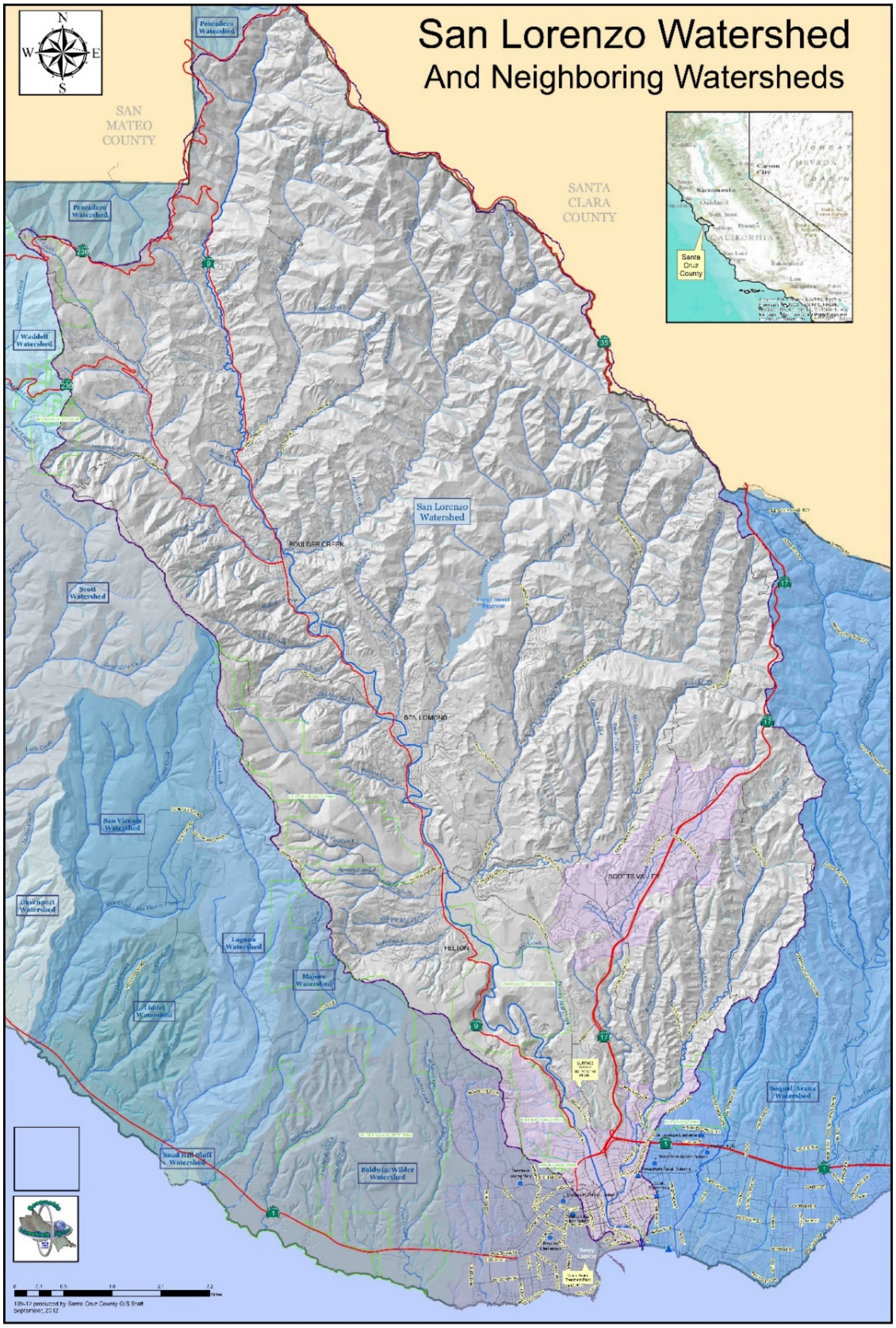

Figure 3. Watershed map of the Santa Cruz region in California.

Figure 4. Sampling Sites

Figure 4. Water sampling and in situ measurement locations. (A) Outflow channel. (B) Cascade facies. (C) First pool. (D) Flag pool. (E) Distal-most pools and oncoid sampling site (Boelts et al., 2020).

Figure 5. Ringtail Creek Longitudinal Profile

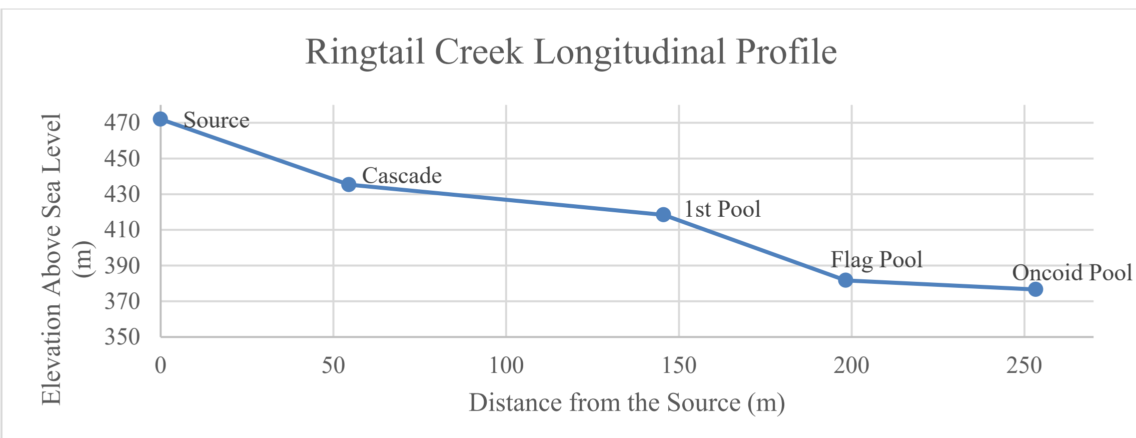

Figure 5. Longitudinal profile of Ringtail Creek in Henry Cowell State Park in Felton, California. The labeled points along the transect are the water collection sites.

Figure 6. Water Temperature

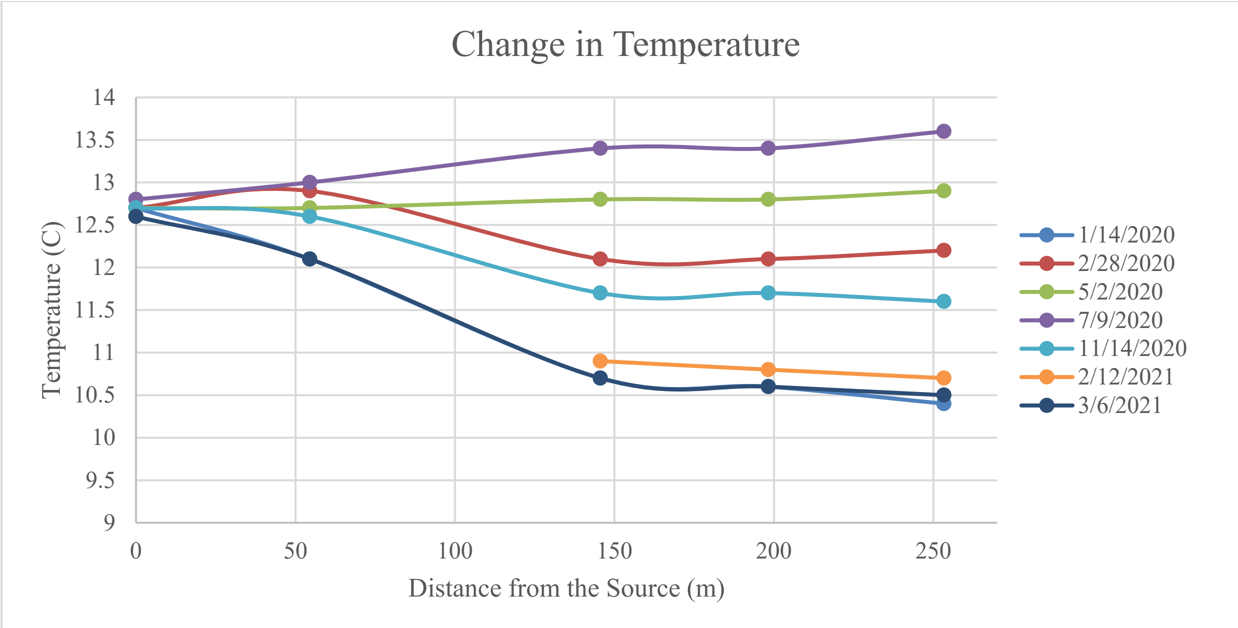

Figure 6. Change in spring water temperature in relation to the distance from the source for different collection dates.

Figure 7. pH

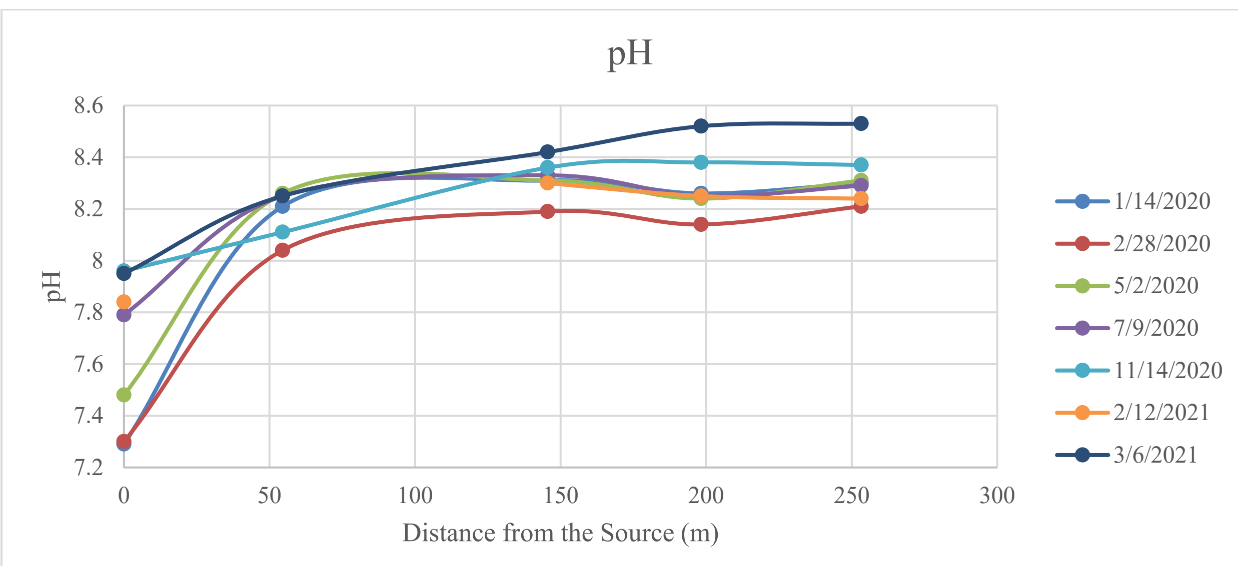

Figure 7. Change in pH in relation to the distance from the source of Ringtail Creek.

Figure 8. pH versus water temperature

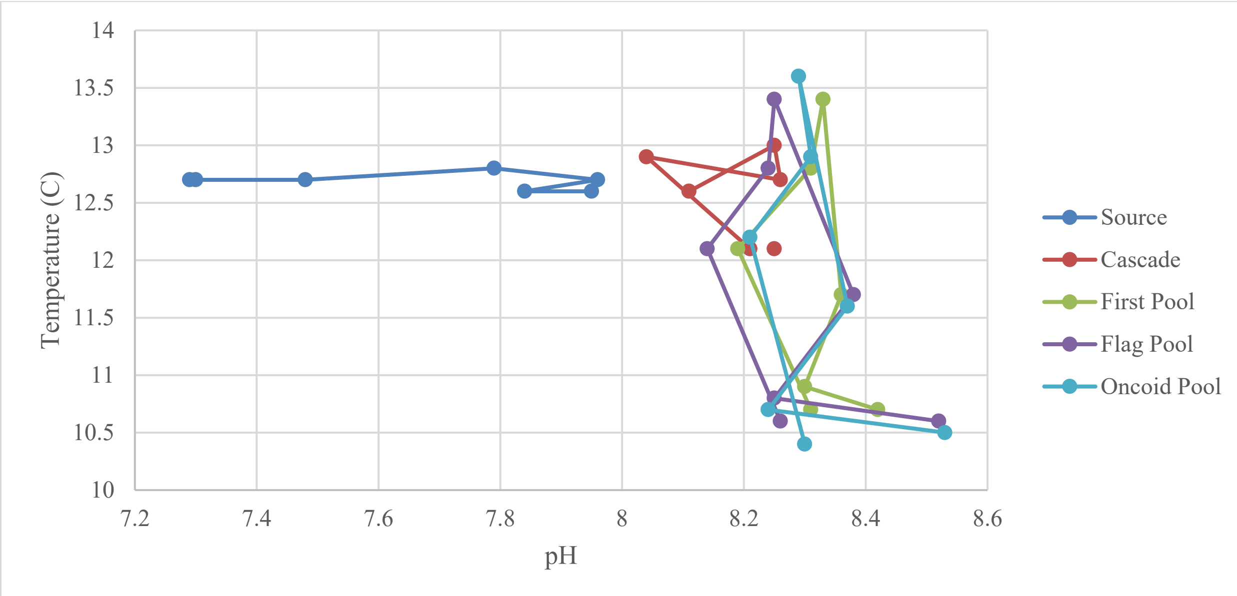

Figure 8. Change in pH versus temperature in relation to the sampling site.

Figure 9. Dissolved Oxygen Content

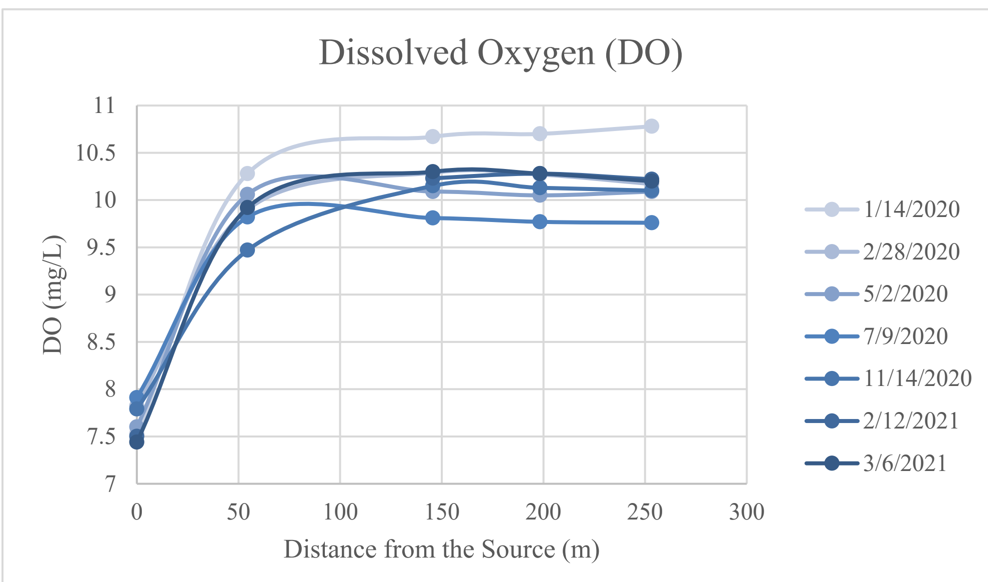

Figure 9. Change in dissolved oxygen (DO) content with distance from the source for different sampling periods.

Figure 10. Oxygen Redox Potential

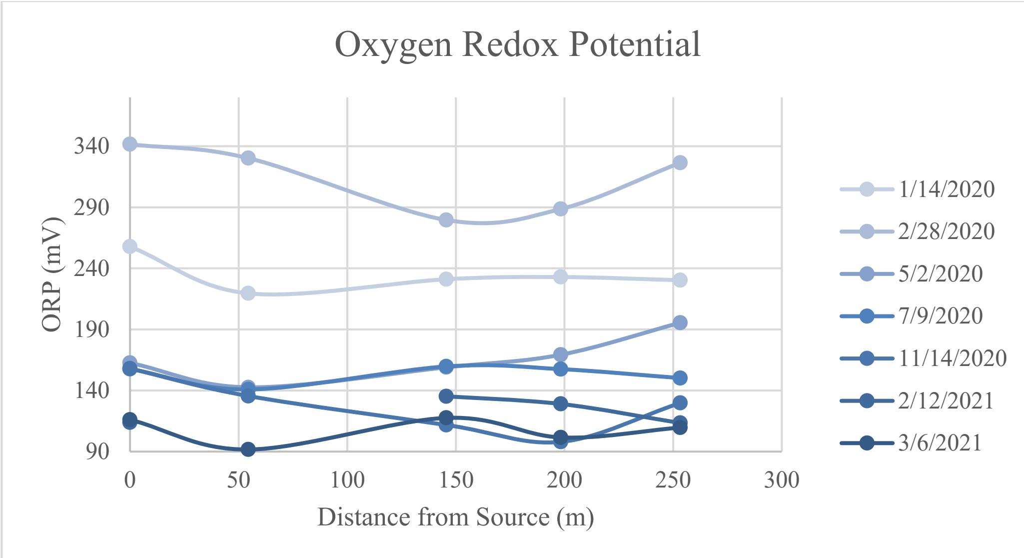

Figure 10. Change in oxygen redox potential (ORP) with distance from from the source for different sampling periods.

Figure 11. Oxygen Redox Potential vs. Sampling date

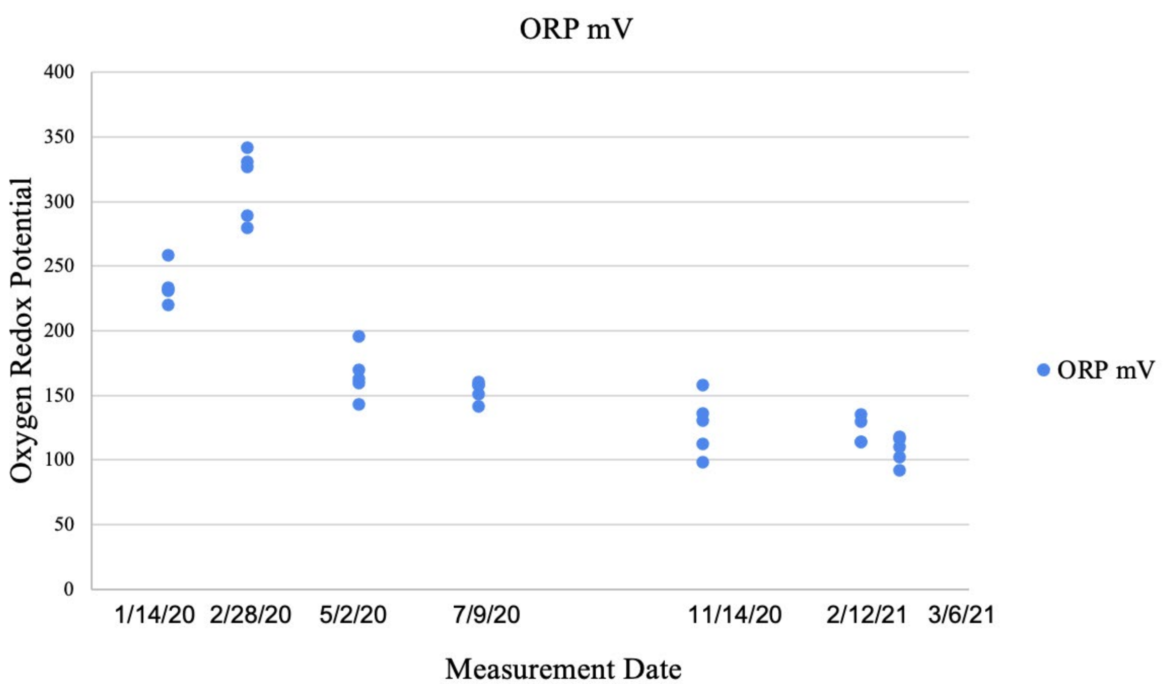

Figure 11. Change in oxygen redox potential (ORP) for each of the sampling dates.

Figure 12. Ca Concentration Over Time

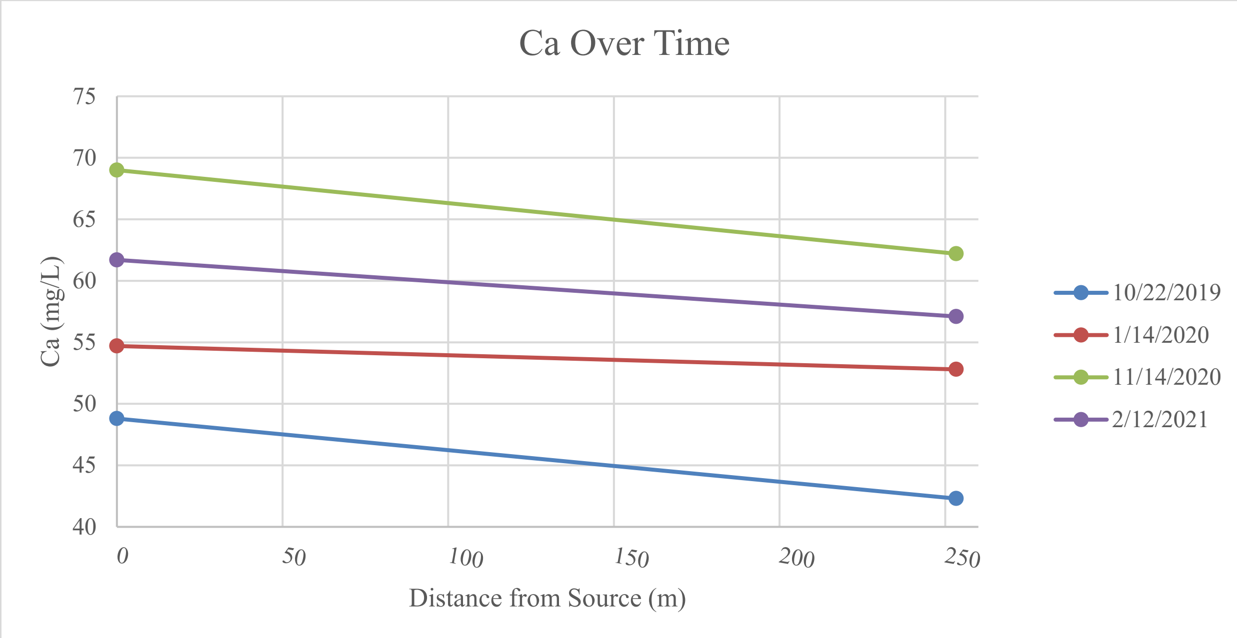

Figure 12. Calcium content over time at the source (left most data points) and the oncoid pool (right most data points).

Figure 13. Cations by site and sampling date

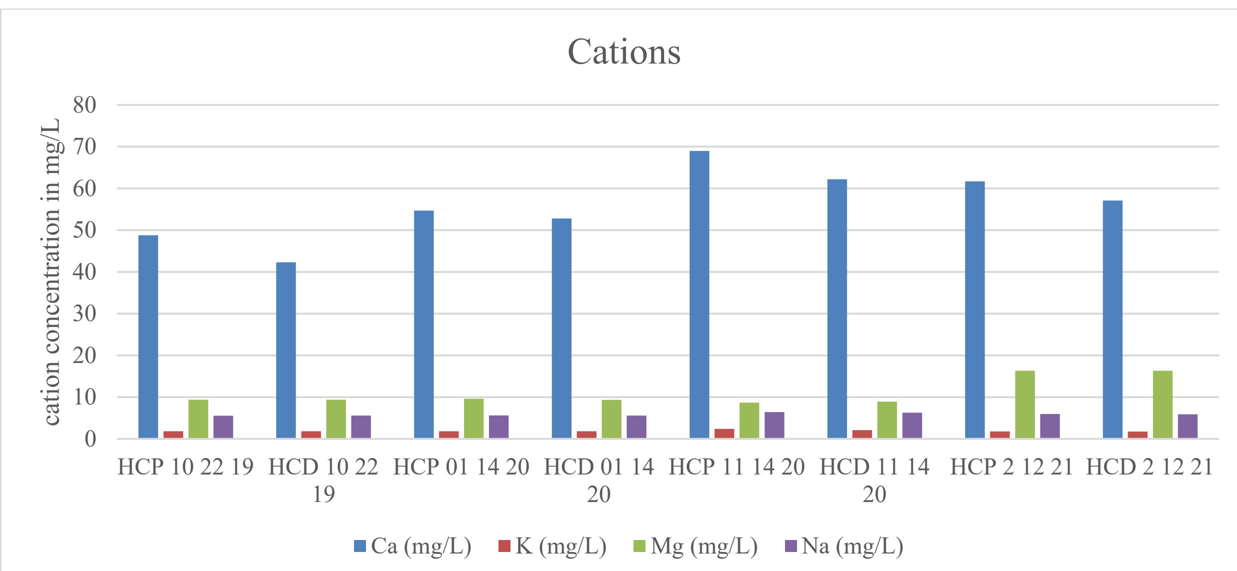

Figure 13. Cation concentration in mg/L of water by site (proximal and distal) and sampling date.

Figure 14. Organic carbon by site and sampling date

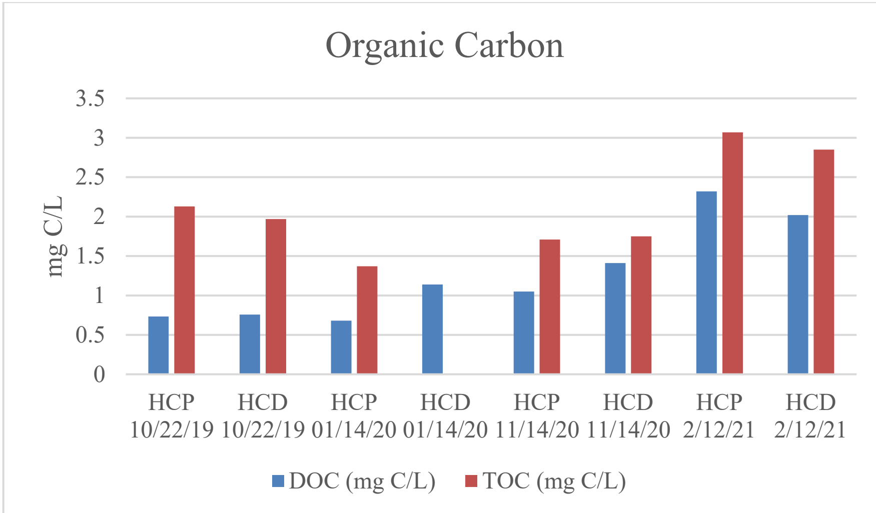

Figure 14. Total and dissolved organic carbon concentrations in mg of carbon per liter of water by sampling location and sampling date.

Figure 15. Piper Diagram

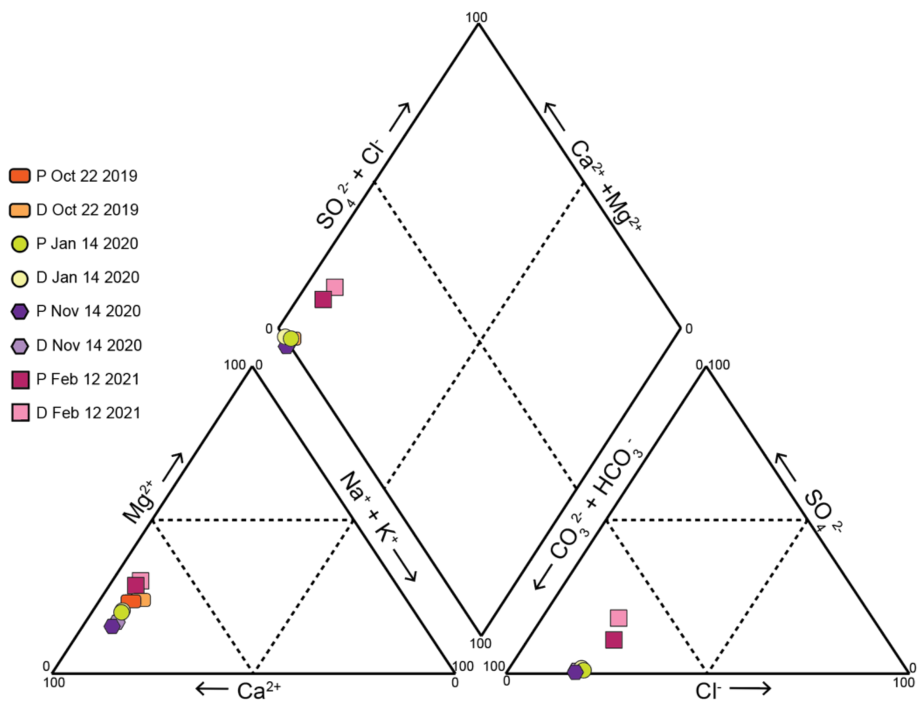

Figure 15. Piper plot of the water samples from Ringtail Creek (2019-2021). "P" samples correspond to the spring source and "D" samples correspond to the distal-most pool.

Figure 16. Silica Over Time

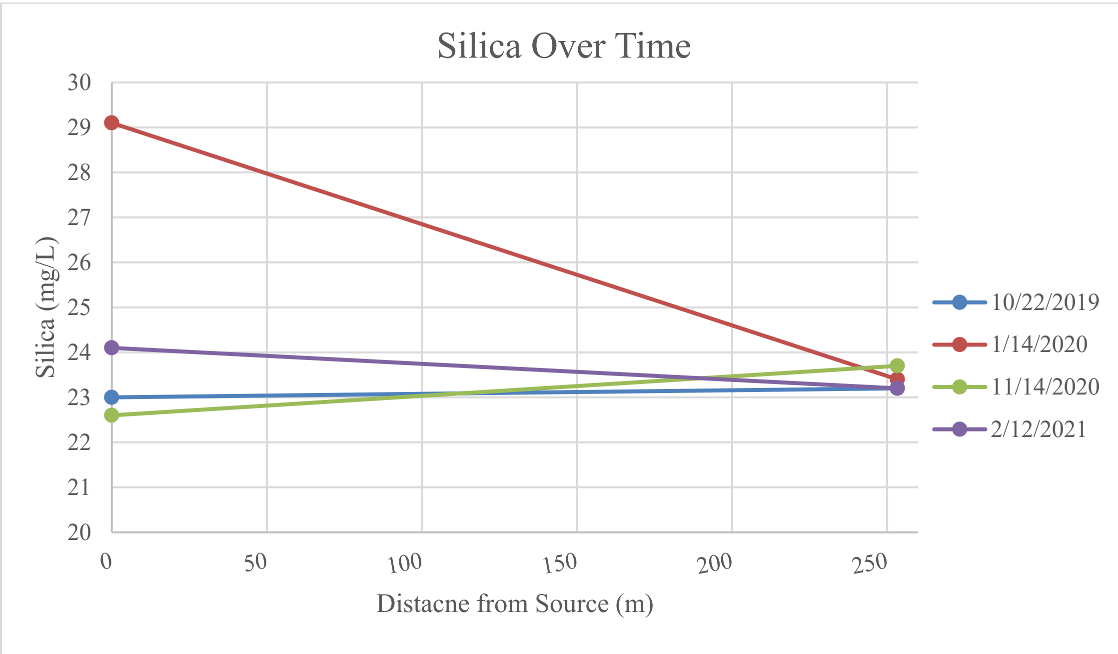

Figure 16. Silica content over time at the source (left most data points) and the oncoid pool (right most data points).

Figure 17. Calcite Saturation Over Time

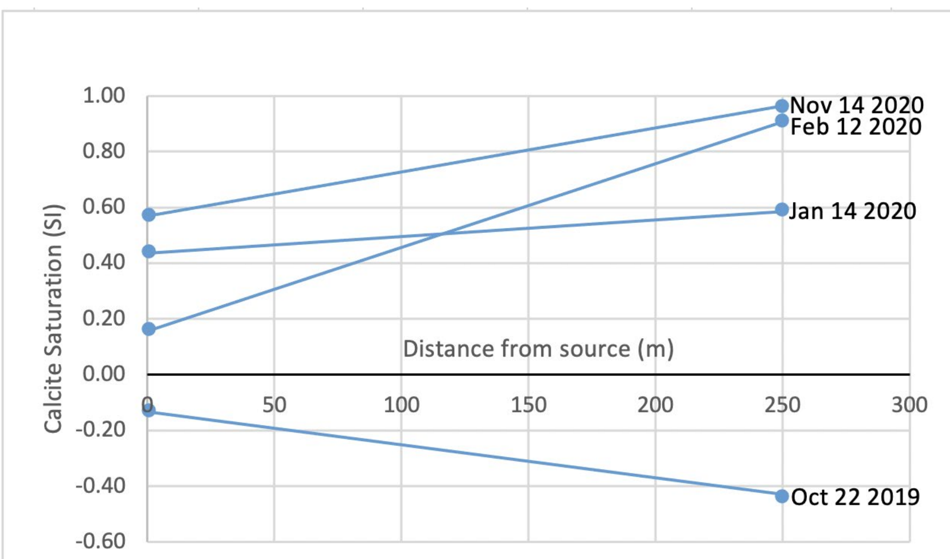

Figure 17. Calcite saturation index (SI) from water samples from Ringtail Creek for the source and distal-most pool.

Figure 18. Post CZU Lightning Complex Fire images

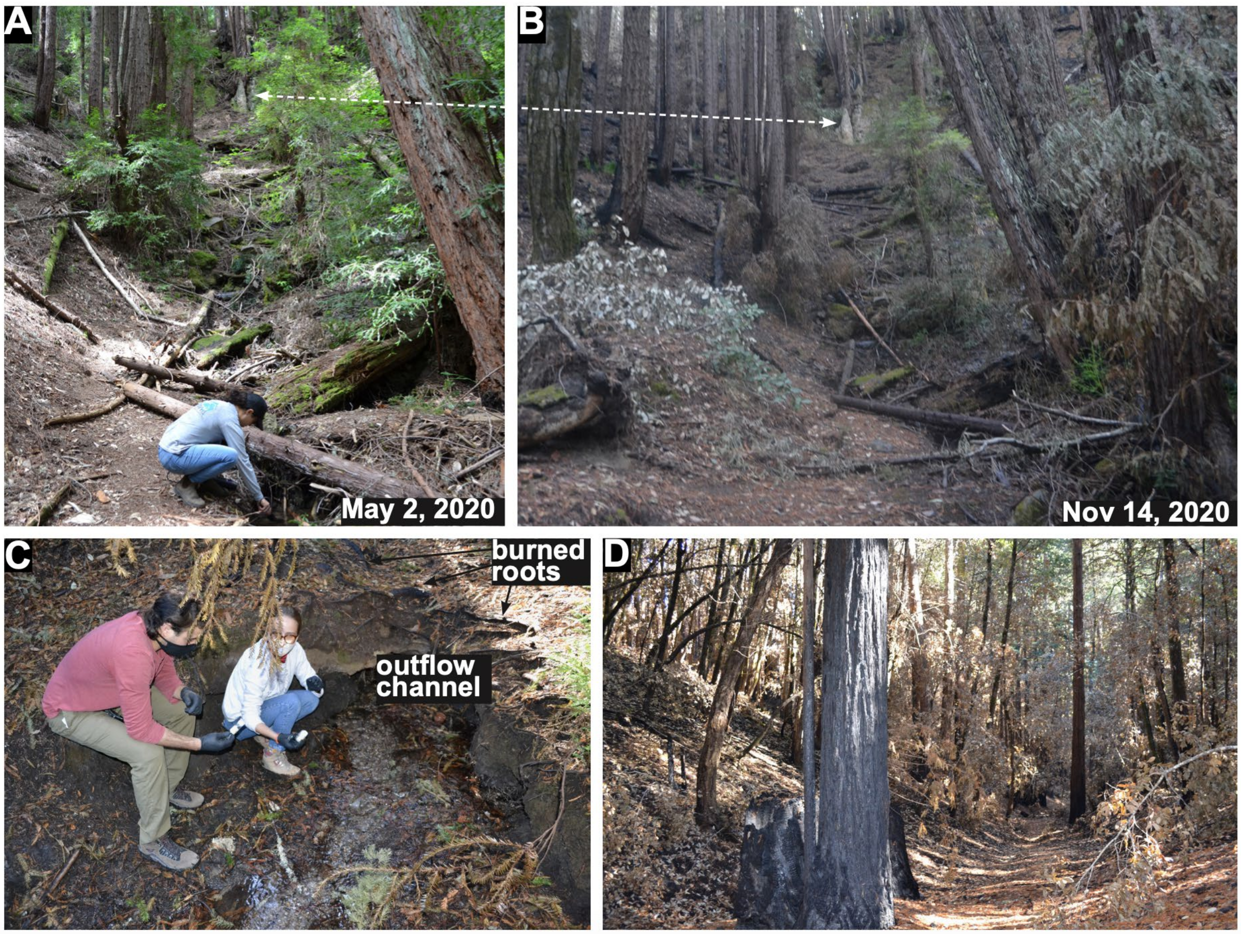

Figure 18. (A-B) Before (A) and after (B)wildfire site photos of a section of the spring transect depicting the effects of the CZU Lightning Complex Fire. (C) Outflow channel post wildfire. (D) Ringtail creek catchment post wildfire (Nov. 14, 2020).

References

Andrews, J.E., 2006, Palaeoclimatic records from stable isotopes in riverine tufas: Synthesis and review: Earth-Science Reviews, v. 75, p. 85–104, doi:10.1016/j.earscirev.2005.08.002.

Arenas, C., Auqué, L., Osácar, C., Sancho, C., Lozano, M. V., Vázquez-Urbez, M., and Pardo, G., 2015, Current tufa sedimentation in a high discharge river: A comparison with other synchronous tufa records in the Iberian Range (Spain): Sedimentary Geology, v. 325, p. 132–157, doi:10.1016/j.sedgeo.2015.05.007.

Arenas, GutiÉrrez, OsÁcar, and Sancho, 2000, Sedimentology and geochemistry of fluvio-lacustrine tufa deposits controlled by evaporite solution subsidence in the central Ebro Depression, NE Spain: Sedimentology, v. 47, p. 883–909, doi:10.1046/j.1365-3091.2000.00329.x.

Arenas, C., Vázquez-Urbez, M., Auqué, L., Sancho, C., Osácar, C., and Pardo, G., 2014, Intrinsic and extrinsic controls of spatial and temporal variations in modern fluvial tufa sedimentation: A thirteen-year record from a semi-arid environment: Sedimentology, v. 61, p. 90–132, doi:10.1111/sed.12045.

Boelts, H.P., Ibarra, Y., and Hayzelden, C., 2020, The influence of benthic diatoms on the textures of carbonate-coated grains from a fluvial tufa spring in northern California: Journal of Sedimentary Research, v. 90, p. 1601–1613, doi:10.2110/jsr.2020.74.

Brasier, A.T., Andrews, J.E., Marca-Bell, A.D., and Dennis, P.F., 2010, Depositional continuity of seasonally laminated tufas: Implications for δ18O based palaeotemperatures: Global and Planetary Change, v. 71, p. 160–167, doi:10.1016/j.gloplacha.2009.03.022.

California Department of Water Resources, 2014,.

Campos, R., Goni, J., Treibs, A., 1977, Advances in Organic Geochemistry: Empresa Nacional Adaro de Investigaciones Mineras,.

Capezzuoli, E., Gandin, A., and Pedley, M., 2014, Decoding tufa and travertine (fresh water carbonates) in the sedimentary record: The state of the art: Sedimentology, v. 61, p. 1–21, doi:10.1111/sed.12075.

Capezzuoli, E., Gandin, A., and Sandrelli, F., 2008, Evidence of associated deposition of travertine and calcareous tufa in the Quaternary carbonates of Valdelsa Basin (Tuscany): Alpine and Mediterranean Quaternary, v. 21, p. 113–124.

Cremaschi, M., Zerboni, A., Spotl, C., and Felletti, F., 2010, The calcareous tufa in the Tadrart Acacus Mt. (SW Fezzan, Libya): AN early Holocene paleoclimate archive in the central Sahara: El Sevier, v. 287, p. 81–94.

David Parkhurst, Apello, C., 2014, Description of Input and Examples for Phreeqc Version 3: Createspace Independent Pub, v. 3.

Ford, T.D., and Pedley, H.M., 1996, A review of tufa and travertine deposits of the world: Earth-Science Reviews, v. 41, p. 117–175, doi:10.1016/s0012-8252(96)00030-x.

Garrett, D.E., 2004, Handbook of Lithium and Natural Calcium Chloride: Elsevier Science,.

Gradziński, M., 2010, Factors controlling growth of modern tufa: Results of a field experiment: Geological Society Special Publication, v. 336, p. 143–191, doi:10.1144/SP336.8.

Gurdak, J.J., 2009, Effects of Climate Variability and Change on Groundwater Resources of the United States. US Geol Surv Fact Sheet 2009-3074: , p. 4.

Gurdak, J.J., Geyer, G.E., Nanus, L., Taniguchi, M., and Corona, C.R., 2017, Scale dependence of controls on groundwater vulnerability in the water–energy–food nexus, California

Coastal Basin aquifer system: Journal of Hydrology: Regional Studies, v. 11, p. 126–138, doi:10.1016/j.ejrh.2016.01.002.

Henrichs, S.M., 1987, Organic geochemistry of natural waters (E. M. Thurman [cd.]): Limnology and Oceanography, v. 32, p. 1015–1016, doi:10.4319/lo.1987.32.4.1015b.

Ibarra, Y., Corsetti, F.A., Feakins, S.J., Rhodes, E.J., and Kirby, M.E., 2015, Fluvial tufa evidence of Late Pleistocene wet intervals from Santa Barbara, California, U.S.A.: Palaeogeography, Palaeoclimatology, Palaeoecology, v. 422, p. 36–45, doi:10.1016/j.palaeo.2015.01.012.

Ibarra, Y., and Sanon, S., 2019, A freshwater analog for the production of Epiphyton-like microfossils: Geobiology, v. 17, p. 510–522, doi:10.1111/gbi.12341.

Kano, A., Okumura, T., Takashima, C., and Shiraishi, F., 2019, Geomicrobiological Properties and Processes of Travertine With a Focus on Japanese Sites:

Kawai, T., Kano, A., and Hori, M., 2009, Geochemical and hydrological controls on biannual lamination of tufa deposits: Sedimentary Geology, v. 213, p. 41–50, doi:10.1016/j.sedgeo.2008.11.003.

Kellman, K., 2003, A CATALOG OF THE MOSSES OF SANTA CRUZ COUNTY, CALIFORNIA: , p. 61–82.

Kokh, S.N., Sokol, E. V., Deev, E. V., Ryapolova, Y.M., Rusanov, G.G., Tomilenko, A.A., and Bul'bak, T.A., 2017, Post-Late Glacial calcareous tufas from the Kurai fault zone (Southeastern Gorny Altai, Russia): Sedimentary Geology, v. 355, p. 1–19, doi:10.1016/j.sedgeo.2017.04.003.

Kumar, K., Rawat, D.S., and Joshi, R., 1997, Chemistry of springwater in Almora, Central

Himalaya, India: Environmental Geology, v. 31, p. 150–156, doi:10.1007/s002540050174.

Minissale, A., Kerrick, D.M., Magro, G., Murrell, M.T., and Paladini, M., 2002, Minissale_2002_Geochemistry of Quaternary travertines in_Earth and Planetary Science Letters: v. 203, p. 1–20, papers3://publication/uuid/62157874-B9D6-4EDF-889D-19CC930F0491.

Pentecost, A., 2005, Travertine:

Pfister, L., Wetzel, C.E., Klaus, J., Martínez-Carreras, N., Antonelli, M., Teuling, A.J., and McDonnell, J.J., 2017, Terrestrial diatoms as tracers in catchment hydrology: a review: Wiley Interdisciplinary Reviews: Water, v. 4, p. e1241, doi:10.1002/wat2.1241.

Rabassa, J., 2021, Advances in Geomorphology and Quaternary Studies in Argentina: Proceedings of the Seventh Argentine Geomorphology and Quaternary Studies Congress, v. 7.

Swart, P.K., 2015, The geochemistry of carbonate diagenesis: The past, present and future: Sedimentology, v. 62, p. 1233–1304, doi:10.1111/sed.12205.

White, W.B., 2010, Springwater geochemistry: Elsevier Inc., 231–268 p., doi:10.1016/B978-1-85617-502-9.00006-2.